Project 3: Geometrical Optics

Gianfranco Grillo

October 16th, 2017

Abstract

We present the results of a series of optical experiments involving thin lenses and Gaussian beams. We verify the thin lens equation, estimate the focal length of a plano-convex lens and a plano-concave lens in different ways, find the minimum beam radius and the divergence of a laser beam, expand the beam using a Galilean expander and a Keplerian expander, and attempt to build a shadowgraphy system for visualizing small changes in the refractive index of a medium. We find good agreement between the focal lengths as given by the lenses' manufacturer and those calculated using the thin lens equation. The focal length of the convex lens with a nominal value of 10 cm was measured to be 10.16 ± 0.06 cm, and the focal length of the concave lens with a nominal value of -2.5 cm was measured to be -2.8 ± 1.0 cm. We find a minimum radius for the laser beam of 0.34 ± 0.08 mm and a divergence of 1.22 ± 0.04 mrad, which is consistent with the typical values for HeNe lasers. Our attempts to build the beam expanders were only partially successful, and we were unable to construct the shadowgraphy system.

1 Introduction

Even though classical electromagnetism describes light as a wave phenomenon, the fact that visible light's wavelength ranges from 400 to 700 nm implies that the effects arising from its wavelike nature are often very small, and that a good first approximation to light's behavior can be made by modelling it as if it consisted of rays. Optics performed under this framework, which is mathematically equivalent to the description of a wave with zero wavelength (or infinite frequency), is known as geometrical optics. Treating light as a wave of zero wavelength significantly simplifies the analysis of its propagation, because it allows us to completely ignore diffractive effects. We can describe simple optical systems involving convex and concave lenses, as well as mirrors, from a geometrical optics perspective, by thinking about the light emerging from an object as a multitude of rays that pass through the lenses and bounce off the mirrors in different ways depending on the shape of the lenses and mirrors. This approximation is especially useful when analyzing the propagation of a laser beam through an optical system, because the nature of the laser beam ensures that in certain contexts it can be treated as a single ray of light propagating through space and time. We work under this framework during the first half of our project.

On the other hand, it is also true that the beam emitted by a laser is not exactly equivalent to a ray of light, because it has a non zero width that changes as it propagates, although it does so at a rate that is much less than that of, for example, the beam emerging from a flashlight. We take a closer look at these properties of a laser beam in the second half of our project.

We perform the data analysis using Python and the associated libraries NumPy and SciPy ([1]), as well as the Uncertainty package ([2]).

2 Theoretical background

2.1 Thin lenses

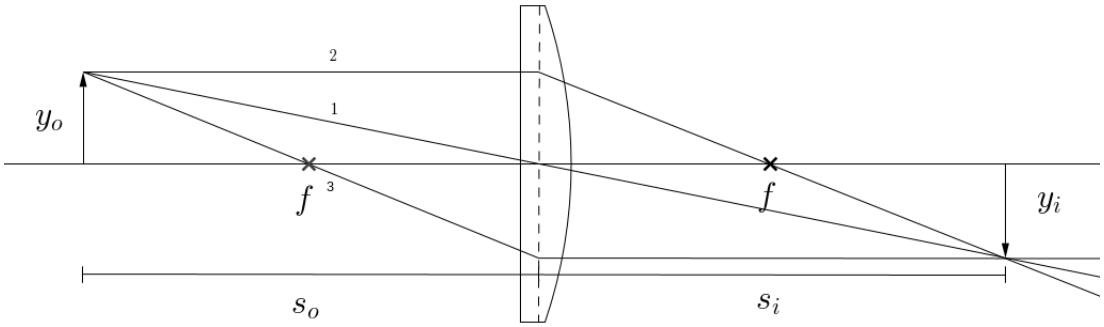

Figure 1: Principal ray diagram for a plano-convex thin lens.

A thin lens corresponds to a lens for which the distance between its front and back interfaces can be neglected without introducing significant errors in the description of ray propagation. As shown in Figure 1 for the case of a plano-convex lens, a simple system made up of an object in front of a thin lens can be described by the parameters s_o, s_i, and f, which correspond to the object distance, the image distance, and the lens's focal length, respectively. These three quantities are related by the thin lens equation

$$\frac{1}{s_o} + \frac{1}{s_i} = \frac{1}{f} \tag{1}$$

The transverse magnification M_T, defined as the ratio of the image height y_i to that of the object height y_i is given by

$$M_T = \frac{y_i}{y_o} = -\frac{s_i}{s_o} \tag{2}$$

A negative magnification implies that the image is inverted, whereas a positive magnification corresponds to an erect image. All real images formed by an optical system composed by a single thin lens will be inverted, because the quantities s_i and s_o are always positive for real objects and images. As shown in the figure, we can calculate the magnification and the image distance of an object if we know the object's distance from the lens and the lens's focal length by drawing a ray parallel to the axis that emerges from the top of the object, passes through the lens and then crosses the focal point to the right of the lens, and another ray that emerges from the same point and then passes through the center of the lens without being deviated. The point at which these two rays intersect corresponds to the position of the top of the image. This sort of ray tracing technique can be very useful when applied to more complicated systems involving more than one lens. Convex lenses have a positive focal length, whereas concave lenses have a negative focal length. This implies that concave lenses are divergent, and convex lenses are convergent.

Systems consisting of more than one lens can be used as beam expanders, because they have a magnification greater than 1. Two types of beam expanders are the Galilean beam expander and the Keplerian beam expander. The Galilean beam expander consists of a diverging lens of focal length f_1

and a converging lens of focal length f_2 separated by a distance $d = f_1 + f_2$, as shown in Figure 2. The magnification of such a system is given by

$$M_G = \frac{-f_2}{f_1} \tag{3}$$

The Keplerian beam expander, on the other hand, consists of two convex lenses, separated by a distance of $d = f_1 + f_2$. This is shown in Figure 3. Note that this distance will be in general greater than that of the Galilean expander because now both focal lengths are positive. The magnification of this system is given by

$$M_K = \frac{f_2}{f_1} \tag{4}$$

We will attempt to build both types of expanders in the last part of this project.

2.2 Ray transfer matrices and the paraxial approximation

A very useful way to describe the propagation of a ray is via the use of ray transfer matrices. In the context of laser optics, this approach can also be made simpler by working under the so-called paraxial approximation. If the object and image distances are large with respect to the transverse size of the lenses used in the optical system, the angle at which a ray can emerge from an object has to be small in order for the ray to pass through the lens as it propagates. This allows us to use the small-angle approximation, where $\sin\theta \approx \tan\theta \approx \theta$, and implies that we can assume that the rays are very close to parallel to the optical axis: they are paraxial. Under this framework, we can relate the height y and the angle θ of a ray with respect to the optical axis via the equation

$$\begin{bmatrix} y \\ \theta \end{bmatrix} = \begin{bmatrix} A & B \\ C & D \end{bmatrix} \begin{bmatrix} y_0 \\ \theta_0 \end{bmatrix} \tag{5}$$

where the matrix is known as the ray transfer or ABCD matrix, and y_0, θ_0 correspond to the initial height and angle of the ray. The components of the matrix depend on the specific structures through which the ray travels. For the purposes of this project, it is enough to introduce the ABCD matrices for a ray travelling a distance d through free space, and a ray crossing a thin lens of focal length f. These are given by

$$M_{FS} = \begin{bmatrix} 1 & d \\ 0 & 1 \end{bmatrix} \tag{6}$$

$$M_{TL} = \begin{bmatrix} 1 & 0 \\ -1/f & 1 \end{bmatrix} \tag{7}$$

The transfer matrix of a ray travelling through a combination of structures can be found by multiplying the matrices of each of these structures.

2.3 Gaussian waves

2.3.1 General definitions

The amplitude of the electric field of the light emitted by a laser can be successfully described by a Gaussian distribution. Following the descriptions given in [3] and [4], we can write the absolute value

of the normalized electric field amplitude of a laser beam propagating in the z-direction as

$$\left|\frac{E(x,\,y,\,z)}{E_0}\right| = \frac{w_0}{w(z)}\exp\left(-\frac{r^2}{w^2}\right) \tag{8}$$

where$w$ corresponds to the beam waist, defined as the point in which the field is down by e^{-1} with respect to the field's strength at $r = 0$, and $w_0 = w(z_0)$, which corresponds to the minimum value of the beam waist. The intensity of the beam as a function of the distance from the beam center is proportional to the square of the electric field, and is thus given by

$$I = I_0\exp\left(\frac{-2r^2}{w^2}\right) \tag{9}$$

where $I_0 = \frac{w_0^2}{w(z)^2}$. The evolution of the beam waist as a function of z is related to the minimum radius w_0 by

$$w(z) = w_0\sqrt{1+\left(\frac{z-z_0}{z_R}\right)^2} \tag{10}$$

where z_R corresponds to the Rayleigh range,

$$z_R = \frac{\pi w_0^2}{\lambda} \tag{11}$$

with λ being the wavelength of the light. Equation (10) can be rewritten in terms of the beam diameter $D = 2w$ and related to the far field divergence angleΘ by the equation

$$D(z) = \sqrt{D_0^2 + [\Theta(z-z_0)]^2} \tag{12}$$

Far away from the beam waist, when $z - z_0 \gg z_R$, Θ approaches $\frac{2w(z)}{z-z_0}$, and it follows that

$$\Theta = \frac{2\lambda}{\pi w_0} \tag{13}$$

Equation (13) will provide a useful check on our measurements. This equation is also a manifestation of Liouville's theorem in optics. This theorem asserts that the phase space volume of system is conserved, which in this context means that the product of the divergence and the beam waist is always equal to a constant.

2.3.2 Calculating the beam size

Since the beam size of a laser is very small, it is not possible to measure small variations in its size by measuring its diameter using a ruler. Instead, we do this by observing how the beam intensity changes as we block part of the beam. If the size of the spot is small compared to the collecting area of the photosensor, the total intensity can be approximated as

$$I_{tot} = \int_{-\infty}^{\infty} I_0 e^{-2r^2/w^2}dr \tag{14}$$

Blocking half of the beam (in this context, using a razor blade) results in an intensity of $I_{1/2} = \frac{I_{tot}}{2}$. If we now translate the razor blade a horizontal distance Δx such that the recorded intensity becomes

a quarter of the original intensity, $I_{1/4} = \frac{I_{tot}}{4} = \frac{I_{1/2}}{2}$, we can find the value of w by solving the following equation:

$$\frac{I_{1/2}}{I_{1/4}} = \frac{\int_0^\infty I_0 e^{-2r^2/w^2} dr}{\int_{\Delta x}^\infty I_0 e^{-2r^2/w^2} dr} \tag{15}$$

$$= \frac{\int_0^\infty e^{-2r^2/w^2} dr}{\int_0^\infty e^{-2r^2/w^2} dr - \int_0^{\Delta x} e^{-2r^2/w^2} dr} \tag{16}$$

Since the LHS of this equation is equal to 2, we can write this as

$$\frac{1}{2} = 1 - \frac{\int_0^{\Delta x} e^{-2r^2/w^2} dr}{\int_0^\infty e^{-2r^2/w^2} dr} \tag{17}$$

Using the solution of the Gaussian integral and solving for w gives

$$w = \frac{\Delta x \sqrt{2}}{\operatorname{erf}(1/2)} \tag{18}$$

We can use (18) to calculate the spot size when we are not too far away from w_0, but measuring the beam's divergence Θ is better done far away from w_0, where the spot size becomes comparable to the size of the photosensor's collecting area. In that case, (18) ceases to be accurate. A better approximation can be performed by taking into account the photosensor's shape and size. For a square photosensor with side length $2a$, the measured intensity when half of the beam is blocked is (assuming the sensor is positioned right behind the razor blade)

$$I_{1/2} = I_0 \int_0^a e^{-2x^2/w^2} dx \int_0^{2a} e^{-2y^2/w^2} dy \tag{19}$$

Translating the razor a horizontal distance Δx such that the new intensity is half of $I_{1/2}$, we see that this new intensity is given by

$$I_{1/4} = I_0 \int_{\Delta x}^a e^{-2x^2/w^2} dx \int_0^{2a} e^{--2y^2/w^2} dy \tag{20}$$

Dividing this two expressions gives

$$\frac{I_{1/2}}{I_{1/4}} = \frac{\int_0^a e^{-2x^2/w^2} dx}{\int_{\Delta x}^a e^{-2x^2/w^2} dx} = 2 \tag{21}$$

We use the solution to the Gaussian integral again to get

$$\operatorname{erf}\left(\frac{a\sqrt{2}}{w}\right) - 2\operatorname{erf}\left(\frac{\Delta x \sqrt{2}}{w}\right) = 0 \tag{22}$$

This equation needs to be solved numerically for w, since it is not possible to solve it analytically. There is very little difference between the values for w obtained for a given Δx using equation (18) and those obtained using (22) when Δx is small compared to a, but the differences become noticeable once Δx gets bigger, which occurs when we measure the beam diameter far away from w_0.

2.4 Shadowgraphy and Schlieren photography

In some engineering applications, especially in fluid dynamics and aerospace engineering, it is very useful to observe the way fluids flow and how they are affected by the presence of an object and changes in their temperature. This can be done by setting up a system that allows one to indirectly observe changes in the refractive index of the fluid. The most basic of these systems is the shadowgraph, and a more advanced one is the Schlieren system. Both systems rely on the fact that that the refractive index of a fluid is related to its density in such a way that a fluid with non-uniform density also has a non-uniform refractive index. The shadowgraph is able to capture these density differences by shining light through the medium and looking at the shadow cast by it due to refraction. In such a system, the observed light intensity is proportional to the Laplacian of the fluid's density. On the other hand, the more sophisticated Schlieren system is similar to the shadowgraph but also utilizes a focusing element and a knife edge in order to take advantage of the fact that the non-uniformity of the fluid results in imperfect focusing, and the resulting light intensity is then proportional to the first derivative of the fluid's density. A more quantitative analysis of the shadowgraph and the Schlieren system can be found in [5]. We will attempt to build a shadowgraph and a Schlieren system in the last part of this project.

3 Experimental Set-Up and Results

3.1 Experiment 1A

3.1.1 Set-Up

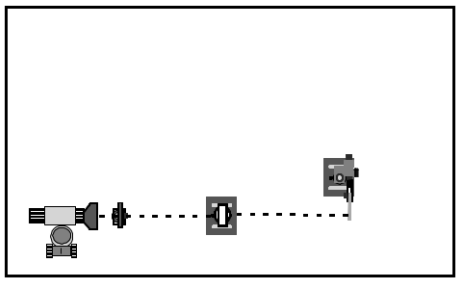

Figure 2: Setup for experiment 1A. Obtained from [6].

In this experiment, we find a lens's focal length by measuring image and object distances, and exploiting the thin lens equation (1). The system setup is shown in Figure 2. We place a flashlight a small distance away from an object with a transparent shape on it, in this case a set of two perpendicular arrows of length 1 cm. Then, we position the lens in front of the object at a distance s_o, and a beam stopper on the other side of the lens. The plano-convex lens is oriented such that its planar surface faces the incoming laser beam in order to reduce aberration. We move the beam stopper into a position that maximizes the sharpness of the arrow image, and take this position to correspond to s_i, the image distance. Finally, we measure the length of one of the arrows in the image and notice its orientation.

3.1.2 Results and analysis

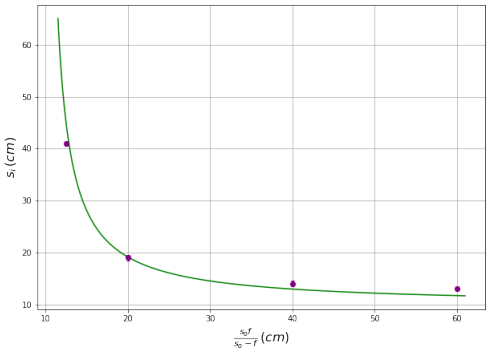

Figure 3: s_i as a function of $s_o$and f, with a best fit using the model given in (23).

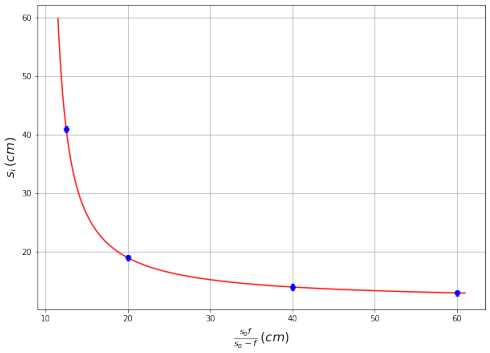

Figure 4: s_i as a function of s_o and f, with a best fit using the model given in (24).

We rearrange equation (1) and write it in the form

$$s_i = \frac{s_o f}{s_o - f} \tag{23}$$

and proceed to fit for f. We also follow another approach in order to account for systematic errors related to the position of the lens principal planes, as well as their precise location within the lens holder, by performing a fit using two auxiliary parameters $\hat{s}_o$ and $\hat{s}_i$ such that

$$s_i = \frac{(s_o + \hat{s}_o) f}{s_o + \hat{s}_o - f} - \hat{s}_i \tag{24}$$

The results of both approaches are shown graphically in Figures 3 and 4. Modelling the data using (23) gives a value for the focal length $f_1 = 9.87 \pm 0.21\,cm$, whereas using equation (24) gives $f_2 = 8.692 \pm 0.005\,cm$, with $\hat{s}_o = -1.247 \pm 0.008\,cm$ and $\hat{s}_i = -2.796 \pm 0.008\,cm$. The standard errors for each of the measurements were taken to be 0.1 cm for s_o and 0.4 cm for s_i, with the larger value for s_i chosen to account for the fact that the beam stopper was not screwed in place and that the sharpness of the image was judged qualitatively.

The value for the focal length given by the simpler model, f_1, is much closer to the value given by the manufacturer of 10 cm. This, together with the relatively large values of $\hat{s}_o$ and $\hat{s}_i$, as well as the small number of data points taken, suggest that the simpler model provides a better estimate of the real focal length of the lens. We do not expect the systematic errors to be as large as the best fit values for $\hat{s}_o$ and $\hat{s}_i$ suggest, because the distance of the principal plane from the lens middle cross section should be very small given that the lens's thickness is very small. We also do not expect the position of the lens holder to affect our results by more than a few millimeters, as anything more than that would be obvious to the naked eye. Thus, it seems that adding those two extra parameters has resulted in an overcorrection that has not improved the accuracy of the results. A better, more detailed model comparison could potentially be done under a Bayesian framework, but this is outside the scope of this work.

$-s_i/s_o$	M	$\%_{dif}$
3.28 ± 0.06	3.00 ± 0.05	8.9
0.95 ± 0.02	1.00 ± 0.05	5.1
0.35 ± 0.01	0.30 ± 0.05	15.3
0.217 ± 0.007	0.15 ± 0.05	36.5

Table 1: Magnification according to (2), measured magnification, and percentage difference between their nominal values.

Table 1 shows a comparison between the theoretical magnification as given by (2) and the actual observed magnification, obtained by dividing the length of one of the object's arrows by the length of the corresponding image arrow. Note that all of the observed images were inverted, which is expected since the object was always placed at a distance larger than the focal length. We can see that three out of the four recorded values agree within their error bars, and the last value is a little off. This is to be expected because for small magnifications, the image size was extremely difficult to measure, since this was done with the naked eye using an ordinary ruler with a scale that had minimum divisions of 1 mm. Thus, measurements of very small images using this method are not reliable.

3.2 Experiment 1B

3.2.1 Set-Up

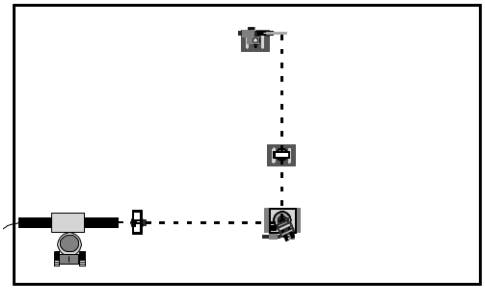

Figure 5: Setup for experiment 1B. Obtained from [6].

This experiment measures object and image distances by a method different than that used in experiment 1A. Instead of using a flashlight, we now use a laser. We place a filter in front of the laser, reducing its intensity by a factor of ~ 3. We then place a mirror on top of a rotation stage in order to deviate the laser beam's path by an angle close to 90°, and place the lens in this direction, with the planar side facing the incident beam in order to minimize aberration effects. We then place a beam stopper behind the lens, and vary its distance until it reaches a position such that the laser spot does not move on the surface of the beam stopper when the mirror is rotated. The distance between the beam stopper and the lens at which this occurs is the image distance s_i, and the distance between the mirror and the lens is the object distance s_o. A graphical representation of this setup is shown in Figure 5. The reason why we are able to identify the image position using this procedure is because in this context we can regard the laser beam as a single ray emerging from a single point in the surface of an object, and geometrical optics requires that all such rays arrive at the same position in the image

plane, as shown in Figure 1. Rotating the mirror is akin to changing the direction of the ray emerging from an object without changing the position from which the ray emerges.

3.2.2 Results and analysis

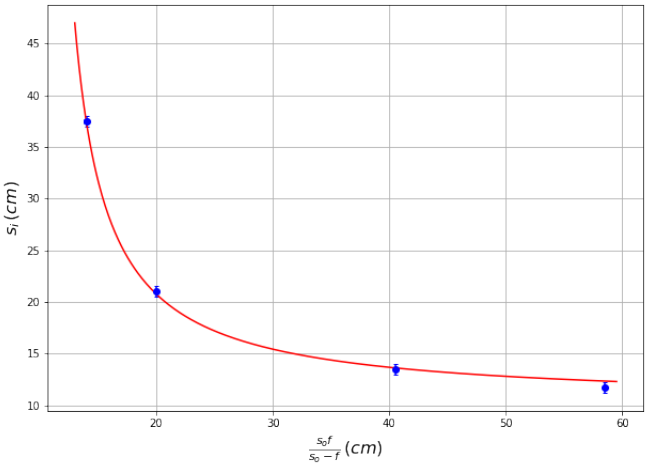

Figure 6: s_i as a function of s_o and f using measurements from experiment 2 and the model given in (23).

Figure 6 shows the results of fitting f to the measurements and the model given in (23). We obtain a value for the focal length of $f = 10.18 \pm 0.06$ cm. We assume a standard error of 0.5 cm for the s_i measurements, and a standard error of 0.2 cm for the s_o measurements. This difference in the assumed standard errors is made in order to partly account for the fact that we are qualitatively judging the beam stopper position that minimizes the movement of the spot as a function of the rotation of the mirror, and this judgment increases the uncertainty in s_i but not in s_o. The result has deceptively small error bars that are not large enough for the measured focal length to be consistent with the 10 cm value given by the manufacturer. This very small error, however, suggests that the measurements were well made, and that the discrepancy does not arise from the judgments made during the procedure; instead, it is suggestive of some form of systematic error. This is further reinforced by the fact that very small changes in the measured values yield results that are a lot closer to the expected values. For instance, subtracting 0.3 cm to each measured value of s_o and s_i gives $f = 10.01 \pm 0.07$ cm. Some degree of systematic error is to be expected since, as mentioned earlier, there are some uncontrolled variables like the position of the lens's principal plane and the lens holder, and in this particular experiment we also have that the point in which the laser strikes the mirror is not directly above any of the table's holes. Finally, alligning the mirror such that its axis of rotation intercepted the point of reflection of the laser was also done qualitatively, which is expected to introduce some degree of systematic error because it implies that rotating the mirror not only changes the angle of the ray that strikes the lens, but also the position from which it emerges with respect to the mirror, which makes the analysis more complicated.

3.3 Experiment 1C

3.3.1 Set-Up

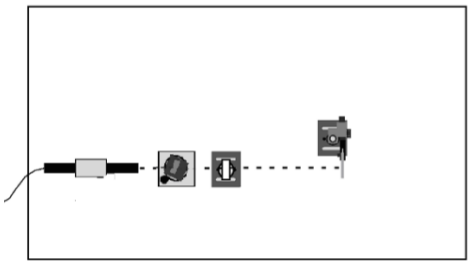

Figure 7: Setup for experiment 1C (i). Obtained from [6].

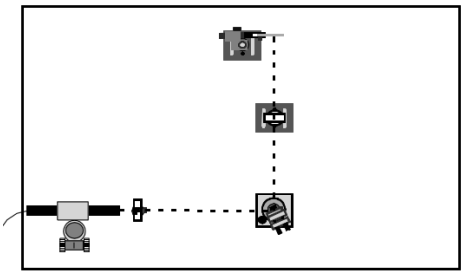

Figure 8: Setup for experiment 1C (ii). Obtained from [6].

We now measure the focal length of the lens in another way by using a glass slab to translate the laser beam. We position the glass slab in front of the laser atop a rotation stage, and place the lens directly in front of it, with the planar side facing the incident beam. We now use a beam stopper to locate the focal length by placing it in a position in which the laser spot does not move when the glass prism is rotated. Rotating the glass prism deviates the beam from its original path because of refraction, but the emerging beam is still parallel to its original direction. In terms of the rays shown in Figure 1, this is essentially equivalent to drawing ray number 2 at different y_o. The only point in the image side of the lens that intersects all incoming parallel rays from the object is the lens's focal point, so this procedure enables us to find the focal length of the lens.

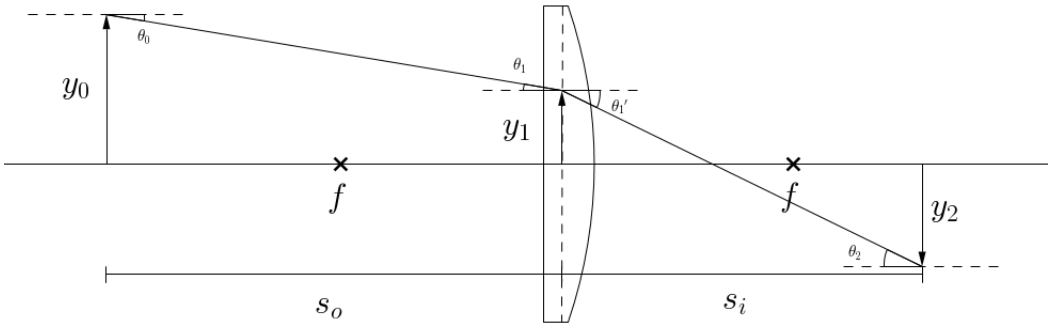

Figure 9: Ray diagram for experiment 1C (ii). Translating the mirror is equivalent to changing y_0, whereas rotating the mirror corresponds to a change in θ_0.

We now switch back to a configuration similar to the one used in experiment 1B, with the difference that now the lens is placed on top of a translation stage and a rotation stage at the same time, as

shown in Figure 8. This enables us to vary both the angle of the ray, as we did in experiment 1B, and the height at which the ray emerges, as we did in 1C (i). The goal is to find the appropriate s_o and s_i such that translating the mirror does not result in any motion of the spot, but rotating the mirror does. Note that in this context, s_i corresponds to the distance between the beam stopper and the lens. A ray diagram for the setup is shown in Figure 9. In terms of the quantities represented on this diagram, translating the mirror corresponds to a change in y_0, and rotating the mirror corresponds to a variation in θ_0. We can use the ray transfer matrix method within the paraxial approximation described in section 2.2 in order to find the necessary conditions that result in y_2 being independent from y_0, but not independent from θ_0. We can relate y_0 and θ_0 to y_2 and θ_2 via the matrix equation

$$\begin{bmatrix} y_2 \\ \theta_2 \end{bmatrix} = \begin{bmatrix} 1 & s_i \\ 0 & 1 \end{bmatrix} \begin{bmatrix} 1 & 0 \\ -1/f & 1 \end{bmatrix} \begin{bmatrix} 1 & s_o \\ 0 & 1 \end{bmatrix} \begin{bmatrix} y_0 \\ \theta_0 \end{bmatrix} \tag{25}$$

$$= \begin{bmatrix} y_0 + \theta_0(s_o + s_i) - \frac{s_i(y_0 + s_o\theta_0)}{f} \\ \theta_0 - \frac{y_0 + s_o\theta_0}{f} \end{bmatrix} \tag{26}$$

In order to find the s_o and s_i that result in y_2 being independent of y_0, we take the derivative of y_2 with respect to y_0 and set it equal to zero:

$$\frac{dy_2}{dy_0} = 1 - \frac{s_i}{f} = 0 \tag{27}$$

Solving for s_i gives

$$s_i = f \tag{28}$$

Taking the derivative of y_2 with respect to θ_0 and using this result, we have

$$\frac{dy_2}{d\theta_0} = s_o + s_i - \frac{s_i s_o}{f} = f \tag{29}$$

These two results imply that the experimental goal can be achieved simply by placing the beam stopper at a distance f from the lens, independently of the value of s_o.

3.3.2 Results and analysis

$s_o\,(\pm 0.2\,cm)$	$f\,(\pm 0.5\,cm)$
10.3	10.5
25.5	10.5
41.0	10.5
66.5	9.5
81.5	9.7

Table 2: Focal length f at different object distances s_o, obtained by applying the procedure described in 3.3.1.

Table 2 shows the results of our measurements for multiple s_o. Combining them, we obtain a value for the focal length of $f = 10.1 \pm 0.4$ cm, which is in agreement with expectations. The large uncertainty assumed for the measurements of f comes again from the nature of the procedure, where we have qualitatively judged the position of the beam stopper that minimizes the spot movement when the

glass slab is rotated. The measured values appear to suggest that f is larger for smaller values of s_o, but it is very hard to draw any conclusions from this small set of observations, given the large error bars and the fact that there does not seem to be any aspect of the experiment that could explain such a relationship. The most likely explanation is that this discrepancy is due to the qualitative nature of the procedure used to measure f.

After performing the measurements, we rotated the lens by 180° in order to see whether the orientation of the plano convex lens changed our observations. We were unable to detect any changes. The orientation of the lens affects the amount of aberration, as mentioned before, but the nature of the laser beam makes it hard to detect blurring associated to aberration effects, especially if the aberration is small.

Measuring f using the setup in 1C (ii) gives a focal length of 11.5 ± 2.0 cm, which is within expectations. We noticed that it was very hard to judge the point in which the y_2 became independent of y_0, as placing the beam stopper anywhere within 2 cm of 11.5 cm resulted in very little spot movement when the mirror was translated. This explains the large value for the uncertainty.

3.4 Experiment 1D

3.4.1 Set-Up

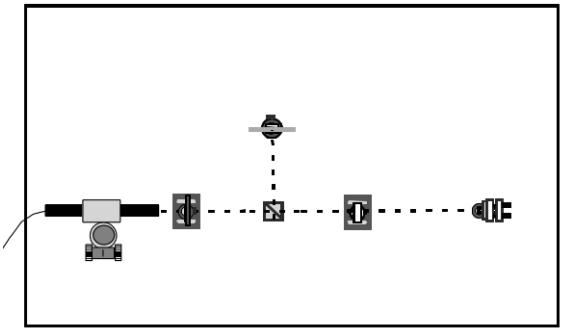

Figure 10: Setup for experiment 1D. Based on original obtained from [6].

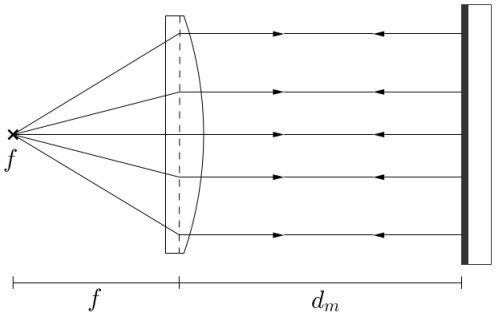

Figure 11: Illustration of the autocollimation effect.

We now measure the focal length of the lens using an autocollimation procedure. We place a pinhole in a filter holder directly to the right of the laser, and position a beam splitter to the right of the pinhole. We then place a flat mirror an appropriate distance away to the right of the beam splitter that enables us to place the lens in between the mirror and the beam splitter. We also position the beam stopper at 90° with respect to the beam splitter, in order to be able to observe the characteristics of the reflected beam. We can measure the focal length by finding the distance from the beam splitter at which we need to place the lens such that moving the mirror back and forth along the direction of propagation does not affect the sharpness of the spot that can be observed at the beam stopper. This distance corresponds to the lens's focal length, because light emerging from a point source that is placed at the focal distance from a convex lens emerges collimated, that is, with rays parallel to each other, so the characteristics of the reflected beam are independent of the mirror's distance from the lens, d_m. This is illustrated in Figure 11.

3.4.2 Results and analysis

Using this method, we obtained a result for the focal length of $f = 10 \pm 2.5$ cm. The uncertainty for this measurement is significantly larger than the one for some of the previous measurements, and the reason is simply that it is extremely hard to judge whether the sharpness of the reflected beam changes or not. We found that we could place the lens up to 2.5 cm away from the 10 cm mark without observing any obvious change in the characteristics of the reflected beam. The procedure is complicated because it is very hard to move the mirror back and forth without misalligning the system, and the brightness of the beam spot is very small given that the original beam needs to pass first through the pinhole and then twice through the beam splitter before hitting the beam stopper.

Combining the results for f found using all the different methods gives a weighted value for the focal length of $f = 10.16 \pm 0.06$ cm, which differs from the expected value by at least 1.0%. This is a reasonable error, given the already mentioned limitations of each of the procedures performed.

3.5 Experiment 2

3.5.1 Set-Up

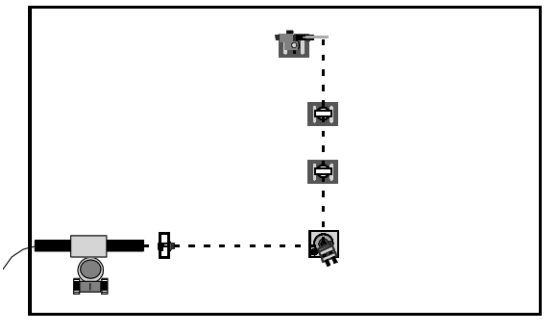

Figure 12: Setup for experiment 2. Obtained from [6].

In this experiment, we measure the focal length f_1 of a plano-concave lens with nominal value of -2.5 cm. The setup is shown in Figure 12. We place an 0.5 ND filter inmediately in front of the laser, and a mirror some reasonable distance away from it. We now place the plano-concave lens with its concave side facing the mirror at a distance s_{o1}, in a position that makes a $\sim 90^\circ$ angle with the original direction of propagation of the beam. Next, we mount a plano-convex lens of focal length $f_2 = 10$ cm in front of the concave lens at a distance $d > 10$ cm. Finally, we place the beam stopper behind the convex lens, and find the image distance of the convex lens s_{i2}using the same procedure as in experiment 1B: by looking for the position of the beam stopper that results in no motion of the beam spot when the mirror is rotated. Based on these measurements, we can calculate f_1 as follows. Using the thin lens approximation, we have the following two equations

$$\frac{1}{f_1} = \frac{1}{s_{i1}} + \frac{1}{s_{o1}} \tag{30}$$

$$\frac{1}{f_2} = \frac{1}{s_{i2}} + \frac{1}{s_{o2}} \tag{31}$$

In addition, we have that s_{i1} is related to d and s_{o2} by

$$s_{i1} = d - s_{o2} \tag{32}$$

Combining (32) with (30) and solving for f_1 gives

$$f_1 = \frac{s_{o1}(d - s_{o2})}{s_{o1} + d - s_{o2}} \tag{33}$$

Finally, solving for s_{o2} in (31) and substituting

$$f_1 = \frac{s_{o1}d(s_{i2} - f_2) - f_2 s_{o1} s_{i2}}{(s_{i2} - f_2)(s_{o1} + d) - f_2 s_{i2}} \tag{34}$$

3.5.2 Results and analysis

We used a distance between the convex and concave lens $d = 20.0 \pm 0.2$ cm, and a distance between the mirror and the concave lens $s_{o1} = 22.8 \pm 0.2$ cm. The measured image distance was $s_{i2} = 18.0 \pm 0.5$ cm, which gives a focal length $f_1 = -2.8 \pm 1.0$ cm. f_1 was taken as 10 ± 0.1 cm. The large value in the uncertainty of s_{i2} derives, as in previous experiments, from the qualitative aspect of the procedure used to determine it. Even though the individual uncertainties of the measured values are not large relative to their nominal value, propagation of the error results in a large uncertainty for the value of f_1, due to the large number of operations that need to be performed between the quantities in order to arrive to the result. This also implies that relatively small changes in the measured value for s_{i2} introduce large variations in the computed value of f_1. For instance, using $s_{i2} = 18.5 \pm 0.5$ cm gives $f_1 = -1.9 \pm 0.8$ cm, and using $s_{i2} = 19 \pm 0.5$ cm yields $f_1 = -1.2 \pm 0.7$ cm. This suggests that this method of measuring the focal length is not very reliable, unless one is able to determine the distances with a large degree of precision.

3.6 Experiment 3A

3.6.1 Set-Up

The objective of this experiment is to measure the beam divergence Θ of the laser by using equation (12). The way we do this is by first finding the parameters D_0 and z_0, and then measuring D as a function of z, in order to fit for Θ. D_0 and z_0 are located inside the laser cavity, so we build a 4-f lens arrangement in order to be able to measure it outside of it. We position a 10 cm plano-convex lens at a distance of 10 cm directly in front of the laser, with its planar side facing the incoming beam. Then we place another 10 cm plano-convex lens at a distance of 20 cm away from the first lens, now with the convex side facing the incoming beam. We adjust the setup slightly so that the beam size, calculated using the procedure described in section 2.3.2 with $a = 1.8\,mm$, is the same right before the first lens and right after the second lens. We set the origin of our coordinate system at the site of the second lens, and measure the beam size relatively close to $z = 0$, looking for the minimum value of D, which corresponds to D_0. The position at which D_0 is found then corresponds to z_0. After finding these two parameters, we extend the laser beam as much as possible using mirrors and measure D as a function of z, and fit for Θ by using the previously measured values of D_0 and z_0.

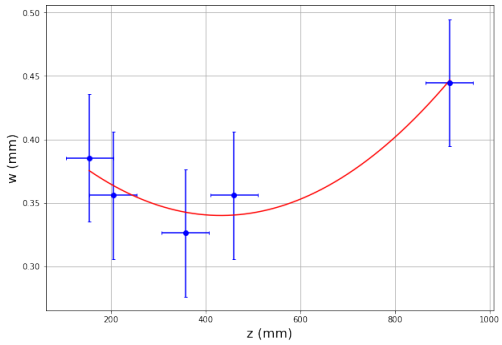

Figure 13: Spot radius w as a function of z near w_0.

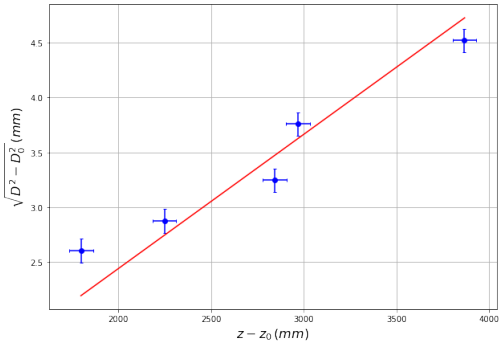

Figure 14: $\sqrt{D^2 - D_0^2}$ vs $z - z_0$ far away from D_0. The slope of the best fit line corresponds to Θ.

3.6.2 Results and analysis

The results of the procedure described above are shown in Figures 13 and 14. The best fit parabola in Figure 13 has a minimum $w_0 = 0.34 \pm 0.08$ mm, which gives a minimum beam diameter of $D_0 = 0.68 \pm 0.16$ mm. This minimum is located at $z_0 = 432 \pm 40$ mm. Equation (12) indicates that plotting $\sqrt{D^2 - D_0^2}$ as a function of $z - z_0$ should result in a straight line with slope Θ. Based on this plot, we obtain a value of $\Theta = 1.22 \pm 0.04$ mrad. According to equation (13), we should also be able to get Θ based only on the value of w_0 and the wavelength of the light, which in this case is equal to $\lambda = 632.8$ nm. Calculating the divergence using this equation gives $\Theta = 1.18 \pm 0.28$ mrad, which is consistent with the measured value. We were unable to find manufacturer information for the particular laser model used, so we cannot compare this value of the divergence with the nominal one, but it is certainly within the range of typical HeNe lasers similar to the one that was used, according to the data found on the manufacturer's site [7].

3.7 Experiment 3B

3.7.1 Set-Up

The goal of this experiment is to build a Galilean beam expander. We place a plano-concave lens of focal length -2.5 cm with its planar side facing the laser, at a distance of 2.5 cm of a plano-convex lens with focal length of 5.0 cm. We adjust this distance slightly such that the beam size right before the plano-concave lens is half of the beam size right after the plano-convex lens, which we expect to hold since the magnification of the system is $M_G = 2$, as per equation (3). We then determine D_0, z_0, and Θ via the same procedure used in experiment 3A.

3.7.2 Results and analysis

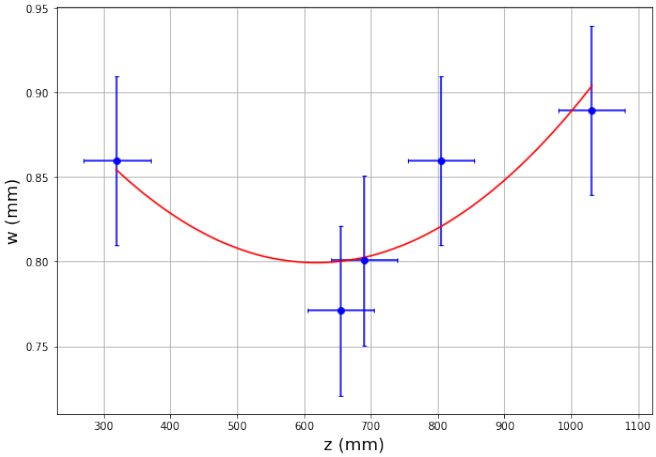

Figure 15: Spot radius w as a function of z near w_0 for the Galilean expander.

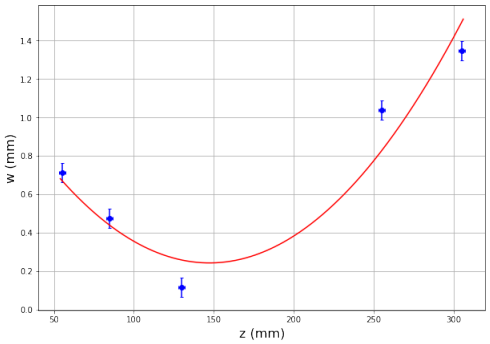

Figure 16: Second set of measurements of spot radius w as a function of z near w_0 for the Galilean expander.

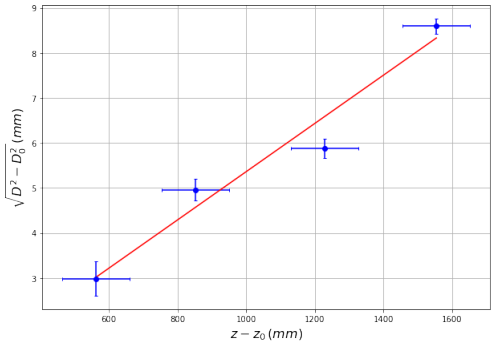

Figure 17: $\sqrt{D^2 - D_0^2}$ vs $z - z_0$ far away from D_0 for the Galilean expander. The slope of the best fit line corresponds to Θ.

The results for this experiment were far from ideal. We were at one point able to correctly setup the expander and measure w_0 and z_0, getting a result of $w_0 = 0.80 \pm 0.30\,mm$ and $z_0 = 620 \pm 50\,mm$, which is not a very accurate result but is consistent with expectations. A plot of the measurements taken is shown in Figure 15. An attempt was made to reproduce the same setup a week later, but the measurements made gave nonsensical results: w_0 was measured to be $0.24 \pm 1.1\,mm$, and $\Theta = 5.4 \pm 0.3\,mrad$, which is roughly 4.5 times the expected value for the divergence if one takes the measured w_0 at face value . These measurements are shown in Figures 16 and 17. No attempt to analyze these results in detail will be made given the obviously faulty nature of the procedure performed. The attempt at building a Keplerian expander by replacing the -2.5 cm lens with a positive lens of 2.5

cm focal length was also unsuccessful, and we will not present the results because they are even more obviously nonsensical than the ones obtained for the Galilean expander.

3.8 Experiment 4

3.8.1 Set-Up

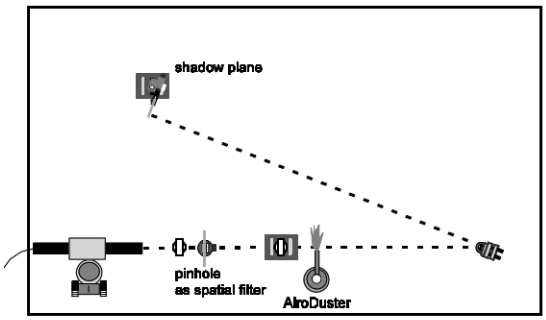

Figure 18: Setup for experiment 4. Obtained from [8].

The procedure for setting up the shadowgraph and the Schlieren system is as follows. We set up a Keplerian beam expander inmediately after the laser, using a pinhole in between the two lenses in order to act as a spatial filter. We place a mirror at the far end of the table in order to increase the distance traveled by the laser beam, and place the AiroDuster in the beam path close to the expander. We then place the beam stopper at about 1.5 m away from the AiroDuster in such a way that it intercepts the beam path. We now squeeze some air out of the AiroDuster, and observe what happens to the image at the target assembly. This setup corresponds to a shadowgraph. In order to transform this into a Schlieren system, we place an additional converging lens in between the mirror and the beam stopper, and place a razor blade at a distance away from the lens equal to the lens's focal length. We then adjust the position of the blade such that the intensity of the light on the screen is half the original intensity of the light on the screen.

3.8.2 Results and analysis

The attempt to build the shadowgraph and the Schlieren system failed. As mentioned before, we were unable to set up the Keplerian beam expander correctly, and it was not possible to construct the shadowgraph without a correctly set up beam expander. In a properly constructed system, we expect that the transition from a shadowgraph to a Schlieren system to increase the sensitivity of the signal because the Schlieren signal is proportional to the first derivative of the air density, and the shadowgraph signal is proportional to the second derivative of the air density, as explained in section 2.4.

4 Conclusions

We have performed a series of experiments in the context of geometrical and Gaussian optics, and exploiting the simplicity of the thin lens approximation. Most experiments were performed correctly

and agreed with expectations, but the last two experiments were not performed correctly. A good way to get better results would be to develop procedures that would enable us to measure certain quantities quantitatively instead of qualitatively; for example, the sharpness of the image in experiment 1A, the movement of the spot in experiments 1B, 1C, and 2, and the sharpness of the reflected beam in experiment 1D. The failure to properly setup the beam expanders has a lot to do with the difficulty in getting the distance between the lenses right, and our equipment was not ideal for the task of slightly adjusting the distance without misalligning the system. It would have been useful to have access to more sophisticated sliders that made this procedure easier.

5 Acknowledgements

The author of this work would like to acknowledge the help received from his lab partner, Juliette Fropier, throughout the data gathering process. I would also like to acknowledge the help provided by our professor, Mukund Vengalattore, and our TA, David Moreau, during lab time.

References

[1] van der Walt, S., et al. *The NumPy Array: A Structure for Efficient Numerical Computation*, Computing in Science & Engineering, 13, 22-30, 2011.

[2] Lebigot, E.O. *Uncertainties: a Python package for calculations with uncertainties*, http://pythonhosted.org/uncertainties/

[3] Hecht, E. *Optics, 5th edit.*, Pearson Education Limited, 2017.

[4] Verdeyen, J. *Laser Electronics, 3rd edit.* Prentice-Hall, Inc., 1995.

[5] Settles, G. S. *Schlieren and Shadowgraph Techniques: Visualizing Phenomena in Transparent Media, 1st edit.*, Springer-Verlag Berlin Heidelberg, 2001.

[6] Bodenschatz, E., et al. *Modern Experimental Optics Laboratory Manual*, Cornell University Physics Department 2016.

[7] IDEX Health & Science. *Random Polarization Products.* 2016. https://www.idex-hs.com/optics/laser-light-sources/helium-neon-lasers/random-polarization.html.